International Journal on Magnetic Particle Imaging
Vol 9, No 1, Suppl 1, Article ID 2303075, 4 Pages

Infinite Science Publishing

Proceedings Article

Single-Pass Relaxation Mapping at Multiple Frequencies Using an Arbitrary Waveform MPI Scanner

Beril Alyuz [1,2,*] · Musa Tunc Arslan [1,2] · Mustafa Utkur [1,2,3,4] · Emine Ulku Saritas [1,2,5]

[1]Department of Electrical and Electronics Engineering, Bilkent University, Ankara, Turkey
[2]National Magnetic Resonance Research Center (UMRAM), Bilkent University, Ankara, Turkey
[3]Harvard Medical School, Boston, MA, United States
[4]Boston Children's Hospital, Boston, MA, United States
[5]Neuroscience Program, Sabuncu Brain Research Center, Bilkent University, Ankara, Turkey
[*]Corresponding author, email: beril@ee.bilkent.edu.tr

Abstract

In Magnetic Particle Imaging (MPI), relaxation behavior of magnetic nanoparticles (MNPs) has enabled the inference of information about different MNP types and their local environments, such as viscosity and temperature. Previously, we have proposed and demonstrated an arbitrary waveform (AW) MPI scanner that facilitates operation in a wide range of drive field (DF) frequencies by eliminating the need for impedance matching. In this work, we propose a technique for simultaneous relaxation mapping at multiple DF frequencies in a single pass using an AW MPI scanner.

I. Introduction

Magnetic nanoparticles (MNPs) have distinct magnetic particle imaging (MPI) signals governed by their physical properties in conjunction with the environmental conditions such as temperature and viscosity, enabling identification of MNP type and environmental properties [1, 2]. We have previously proposed a technique called TAURUS (TAU estimation via Recovery of Underlying mirror Symmetry), a relaxation time constant (τ) estimation method that does not require calibration or prior information about MNPs for distinguishing MNP type or environment [3]. Recently, we have developed Rapid TAURUS, a novel extension of TAURUS that enables τ map estimation for rapid and multi-dimensional trajectories [4].

The MNP signal varies depending on different drive field (DF) parameters, causing the optimal DF parameters to vary depending on the quantitative mapping application [5, 6]. In addition, distinguishing different MNP types or their local environments may require measurements at multiple DF settings [6]. Previous studies employed magnetic particle spectrometer (MPS) setups to achieve arbitrary waveform (AW) characteristics that enable operation at any DF frequency [5, 7–9]. In addition, a small-scale field free line (FFL) MPI scanner was constructed by adding magnets to an AWR to enable pulsed excitation in MPI [10]. We have previously presented a low-inductance DF coil design that eliminates conventional methods for reactive power control and capacitates AW characteristics in a typical-size MPI scanner [11].

In this work, we present a technique for single-pass relaxation mapping at multiple frequencies using an AW MPI scanner. The experimental results are shown through imaging experiments and τ map estimations

with Rapid TAURUS on our in-house FFL AW MPI scanner at two different DF frequencies, 5 kHz and 8 kHz, imaged in a single pass by switching the operating DF back and forth.

II. Methods and Materials

II.I. AW MPI Scanner

Our in-house AW MPI scanner, shown in Fig. 1, features a low-inductance DF coil, wound using Rutherford cable windings [11]. The AW DF coil parameters were optimized to provide a favorable trade-off between coil sensitivity and coil inductance, enabling operation in a wide band of frequencies within the limits of our power amplifier. Accordingly, the AW DF coil has 3 layers with 13 Rutherford cable windings per layer, with each cable having a 6×2 wire structure. The AW DF coil has an inner diameter of 4.4 cm and a length of 12 cm. The inductance of the coil was measured to be around 23.8 µH, with a coil sensitivity of 0.27 mT/A. In contrast, a standard DF coil with the same diameter and length but wound using regular Litz wire windings would have 3.56 mH inductance and 3.28 mT/A coil sensitivity. Hence, the AW DF coil provides lower inductance to enable AW characteristics, at the expense of reduced coil sensitivity.

To ensure that the AW MPI scanner does not cause sample heating due to required high currents, resistive heating over time was simulated in COMSOL Multiphysics ®Version 5.5, utilising a 2D axisymmetric model and implementing Magnetic Fields and Heat Transfer in Solids interfaces with a Frequency-Transient study. The simulations were performed at the targeted DF settings of (f_0, B_{peak})=(5 kHz,15 mT) and (f_0, B_{peak})=(8 kHz,10 mT), for a DF duration of 90 s for each case. The results indicated that no external cooling of the AW DF coil is required, as the temperature change remained negligible after continuously applying the DF for 90 s for both of the DF settings.

A receive coil was designed together with the AW DF coil. It had a three-section gradiometer geometry with 27, 50, and 31 turns for the fixed compensation, center receive, and tuning parts, respectively, achieving around 65 dB decoupling between drive and receive coils. The simulations were done using COMSOL Multiphysics ®Version 5.5. A 2D axisymmetric model was used to model the subcomponents of the AW MPI scanner utilizing the Magnetic Fields interface to simulate the direct feedthrough signal. The optimal number of turns for the fixed compensation and the tuning segment were found with grid search by employing Parametric Sweep study. A homogeneous receive sensitivity profile (> 90% homogeneity) was maintained in a 12.5 mm region at the scanner isocenter.

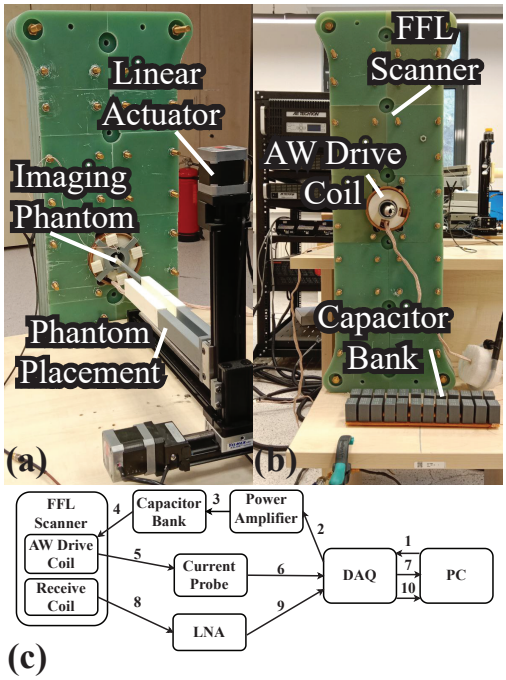

Figure 1: Our in-house AW MPI scanner with an FFL topology. (a) Front and (b) back views of the scanner. The AW DF coil features a low inductance of 23.8 µH. The capacitor bank is used for blocking DC currents on the AW DF coil. (c) Signal flowchart showing the imaging procedure.

III. Experiments

The experiments were performed on our in-house AW MPI scanner. This FFL scanner has selection field gradients of (-4.4,0,4.4) T/m and a free bore diameter of 3.6 cm, capable of performing projection format imaging. Imaging experiments were performed simultaneously at two different DF settings: (5 kHz,15 mT) and (8 kHz,10 mT). The DF waveform was formed by continuously applying 40 periods of a sinusoidal DF at (5 kHz,15 mT) followed by 40 periods of a sinusoidal DF at (8 kHz,10 mT) throughout the total scan time.

The imaging procedure is explained in Fig. 1c. The constructed DF waveform was sent to a power amplifier (AE Techron 7224) through a data acquisition card (DAQ) (NI USB-6383). The power amplifier was directly connected to the AW DF coil without the need for impedance matching. Additionally, a 2×12 capacitor bank was built for blocking DC currents on the AW DF coil, shown in Fig. 1b. Before each experiment, the current through the AW DF coil was calibrated using a current probe (LFR 06/6/300, PEM). The received signal was amplified with a low-noise voltage pre-amplifier (LNA) (SRS SR560) and sent to a PC via the DAQ. The entire setup was controlled using MATLAB.

The imaging phantom contained two samples: 20 µl and 30 µl undiluted Perimag MNPs with 1.7 mgFe/ml

10.18416/ijmpi.2023.2303075

concentration, placed at 4.8 cm separation (see Fig. 2a). For 1D imaging experiments, a linear actuator continuously moved the sample in a line, while the multi-frequency DF waveform was applied simultaneously. A 15 cm field-of-view (FOV) was covered in a total scan time of 7.6 s. All measurements were performed at room temperature.

The overall received signal was separated into two parts, to extract the corresponding signal for each DF setting. Next, MPI images were reconstructed separately at each DF setting using partial FOV center imaging (PCI), a robust x-space based reconstruction algorithm [12]. The τ map estimations were also performed separately at each DF setting, using Rapid TAURUS [4] .

IV. Results and Discussion

The experiment results for the selected DF settings of (5 kHz,15 mT) and (8 kHz,10 mT) are shown in Fig. 2. Imaged in a single pass, both DF settings provided successful MPI image reconstruction and relaxation map estimation. These figures show the percentage τ value with respect to the DF period (i.e., $\hat{\tau} = \tau / T_0 \cdot 100$), to enable comparison of τ from different DF frequencies. Accordingly, while the MPI images look almost identical, $\hat{\tau}$ maps can be easily distinguished between the two DF settings: $\hat{\tau}$ was approximately 2.8% at (5 kHz,15 mT) and approximately 3.2% at (8 kHz,10 mT). This relative change in $\hat{\tau}$ between the two DF settings is consistent with the literature, as $\hat{\tau}$ was shown to increase with increasing DF frequency and decreasing DF amplitude [6].

These results demonstrate that the proposed AW MPI scanner can simultaneously image and estimate τ maps at different frequencies in a single imaging pass, thanks to the operating flexibility that it provides. Note that different MNPs and/or environments may yield identical $\hat{\tau}$ values depending on the DF settings. In addition, environmental factors such as temperature and viscosity may have confounding effects on $\hat{\tau}$ values. Therefore, measurements at two or more DF settings are needed for applications that aim to distinguish different MNP types and their local environments [6]. The proposed approach will be particularly useful for such applications by enabling rapid relaxation mapping at multiple DF settings.

V. Conclusion

In this work, we have presented a relaxation mapping technique at multiple DF frequencies in a single pass using an AW MPI scanner. The low inductance of the AW DF coil enables flexible functionality in a wide range of DF frequencies. Imaging at multiple frequencies in a single pass using the proposed technique provides valuable practicality for quantitative mapping applications of MPI, allowing reduction in scan time for distinguishing MNP types and environmental conditions.

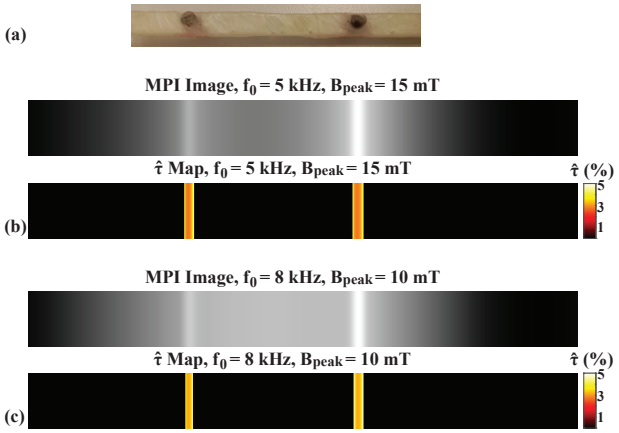

Figure 2: Experiment results at (5 kHz,15 mT) and (8 kHz,10 mT), imaged in a single pass using an AW MPI scanner. (a) Imaging phantom containing two Perimag MNP samples. (b) 1D MPI image and 1D $\hat{\tau}$ map at (5 kHz,15 mT). The estimated $\hat{\tau}$ was approximately 2.8%. (c) 1D MPI image and 1D $\hat{\tau}$ map at (8 kHz,10 mT). The estimated $\hat{\tau}$ was approximately 3.2%. Both the MPI images and $\hat{\tau}$ maps were replicated in the vertical direction for display purposes.

Acknowledgments

This work was supported by the Scientific and Technological Research Council of Turkey (TUBITAK 120E208).

Author's statement

Conflict of interest: Authors state no conflict of interest.

References

[1] A. M. Rauwerdink and J. B. Weaver. Viscous effects on nanoparticle magnetization harmonics. *Journal of Magnetism and Magnetic Materials*, 322(6):609–613, 2010, doi:https://doi.org/10.1016/j.jmmm.2009.10.024.

[2] M. Möddel, C. Meins, J. Dieckhoff, and T. Knopp. Viscosity quantification using multi-contrast magnetic particle imaging. *New Journal of Physics*, 20(8):083001, 2018, doi:10.1088/1367-2630/aad44b.

[3] Y. Muslu, M. Utkur, O. B. Demirel, and E. U. Saritas. Calibration-free relaxation-based multi-color magnetic particle imaging. *IEEE Transactions on Medical Imaging*, 37(8):1920–1931, 2018, doi:10.1109/TMI.2018.2818261.

[4] M. T. Arslan, A. A. Özaslan, S. Kurt, Y. Muslu, and E. U. Saritas. Rapid taurus for relaxation-based color magnetic particle imaging. *IEEE Transactions on Medical Imaging*, 41(12):3774–3786, 2022, doi:10.1109/TMI.2022.3195694.

[5] E. Yagiz, M. Utkur, C. B. Top, and E. U. Saritas. Magnetic particle fingerprinting using arbitrary waveform relaxometer. *International Journal on Magnetic Particle Imaging*, 6(2 Suppl 1), 2020.

[6] M. Utkur and E. U. Saritas. Simultaneous temperature and viscosity estimation capability via magnetic nanoparticle relaxation. *Medical Physics*, 49(4):2590–2601, 2022, doi:https://doi.org/10.1002/mp.15509.

[7] C. B. Top. An arbitrary waveform magnetic nanoparticle relaxometer with an asymmetrical three-section gradiometric receive coil. *Turkish Journal of Electrical Engineering and Computer Science*, 28:1344–1354, 2020, doi:10.3906/elk-1907-201.

[8] Z. W. Tay, P. W. Goodwill, D. W. Hensley, L. A. Taylor, B. Zheng, and S. M. Conolly. A high-throughput, arbitrary-waveform, mpi spectrometer and relaxometer for comprehensive magnetic particle optimization and characterization. *Scientific Reports*, 6(1):34180, 2016, doi:10.1038/srep34180.

[9] D. Pantke, N. Holle, A. Mogarkar, M. Straub, and V. Schulz. Multi-frequency magnetic particle imaging enabled by a combined passive and active drive field feed-through compensation approach. *Medical physics*, 46(9):4077–4086, 2019.

[10] Z. W. Tay, D. Hensley, J. Ma, P. Chandrasekharan, B. Zheng, P. Goodwill, and S. Conolly. Pulsed excitation in magnetic particle imaging. *IEEE transactions on medical imaging*, 38(10):2389–2399, 2019.

[11] B. Alyuz, M. T. Arslan, M. Utkur, and E. U. Saritas. An arbitrary waveform mpi scanner. *International Journal on Magnetic Particle Imaging*, 8(1 Suppl 1), 2022.

[12] S. Kurt, Y. Muslu, and E. U. Saritas. Partial fov center imaging (pci): A robust x-space image reconstruction for magnetic particle imaging. *IEEE Transactions on Medical Imaging*, 39(11):3441–3450, 2020.

